Coherent control of steady-state entanglement in driven cavity arrays

Dimitris G. Angelakis,[1, 2, *] Li Dai,[1] and Leong Chuan Kwek[1, 3]

[1]*Centre for Quantum Technologies, National University of Singapore, 2 Science Drive 3, Singapore 117542*
[2]*Science Department, Technical University of Crete, Chania, Crete, Greece, 73100*
[3]*National Institute of Education and Institute of Advanced Studies,*
Nanyang Technological University, 1 Nanyang Walk, Singapore 637616
(Dated: June 11, 2009)

We show that coherent control of the steady state entanglement between pairs of cavity-atom systems in an array of lossy and driven coupled cavities is possible. The cavities are doped with atoms and are connected through waveguides, other cavities or fibers depending the implementation. We find that the steady state entanglement can be coherently controlled through the tuning of the phase difference between the driving fields. It can also be surprisingly high in spite of the pumps being classical fields. Furthermore, the maximal of entanglement for any pair is achieved when their corresponding direct coupling is much smaller than their individual couplings to the third party. This effect is reminiscent of coherent population transfer through a third level between otherwise uncoupled atomic levels using classical coherent fields. The above results are analyzed for a range of values of the system parameters and different network geometries.

Coupled cavity arrays have recently been proposed as a new system for realizing schemes for quantum computation [1] and for simulations of quantum many-body systems[2]. More recently driven arrays were considered towards the production of steady state entanglement [3] under realistic dissipation parameters. Also, an analogy with Josephson oscillations was shown and the many body properties of the driven array have been recently studied [4].

In this work we examine for the first time the possibility of achieving coherent control of the steady state entanglement. We show explicitly that for a closed geometry for a three-cavity setup, the latter being realizable in a variety of cavity QED technologies including photonic crystals, circuit QED and Fabry-Perot cavities connected through fibers[5, 6, 7, 8], such control is possible (see Fig. 1). Light from the waveguides can directly coupled to the photonic modes of the defects cavities through coherent tunneling. Using the projection operator method and following a similar analysis to that in Ref. [3, 9], we can derive an effective master equation for polaritons in three cavities.

$$\dot{\rho} = -\ i[H_{\text{eff}}, \rho] + \sum_{i=1}^{3} (\frac{\gamma}{2} + \Gamma_i)[2\sigma_i \rho \sigma_i^\dagger - \sigma_i^\dagger \sigma_i \rho - \rho \sigma_i^\dagger \sigma_i]$$
$$+\ \sum_{i=1}^{3} (\frac{\gamma}{2} + \Gamma_i)[2\sigma_{i+1} \rho \sigma_{i+1}^\dagger - \sigma_{i+1}^\dagger \sigma_{i+1} \rho - \rho \sigma_{i+1}^\dagger \sigma_{i+1}]$$
$$+\ \sum_{j=1}^{3} \Gamma_j [2\sigma_j \rho \sigma_{j+1}^\dagger - \sigma_j^\dagger \sigma_{j+1} \rho - \rho \sigma_j^\dagger \sigma_{j+1}$$
$$+\ 2\sigma_{j+1} \rho \sigma_j^\dagger - \sigma_{j+1}^\dagger \sigma_j \rho - \rho \sigma_{j+1}^\dagger \sigma_j] \tag{1}$$

where $\sigma_j^\dagger$ is the polaritonic creation operator for the doped cavities, a, $a^\dagger$ the photon field operators of the
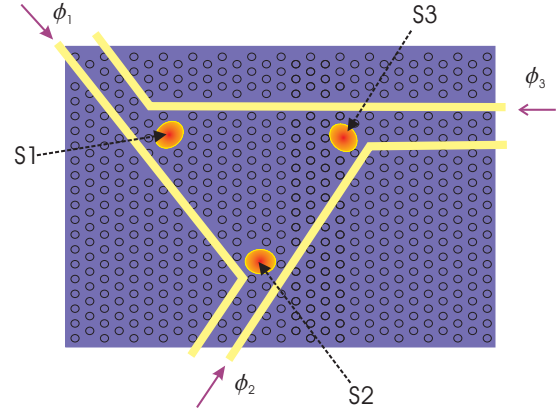

FIG. 1: (color online). Schematic representation of three-doped-defect cavity setup based on a possible implementation using photonic crystals (for illustration purposes only): Each waveguide carrying the driving classical fields can be replaced by fibers in the case of Fabry-Perot cavities or stripline microresonators for circuit QED implementations [5, 6, 7, 8].

central empty cavity and γ, κ the dissipation rates of the polaritonics and the cavity photons.

The effective Hamiltonian is

$$H_{\text{eff}} = -\ \sum_{i=1}^{3} \delta_i (\sigma_i^z + \sigma_{i+1}^z)$$
$$+\ \sum_{i=1}^{3} \frac{J_i^2 \Delta_i}{\kappa^2 + \Delta_i^2} (\sigma_i^\dagger \sigma_i + \sigma_{i+1}^\dagger \sigma_{i+1})$$
$$+\ \sum_{i=1}^{3} \frac{J_i^2 \Delta_i}{\kappa^2 + \Delta_i^2} (\sigma_i^\dagger \sigma_{i+1} + \sigma_{i+1}^\dagger \sigma_i)$$
$$+ \sum_{j=1}^{3} \frac{J_j \alpha_j}{\Delta_j + i\kappa} (\sigma_j^\dagger + \sigma_{j+1}^\dagger) + \sum_{j=1}^{3} \frac{J_j \alpha_j}{\Delta_j - i\kappa} (\sigma_j + \sigma_{j+1}) \tag{2}$$
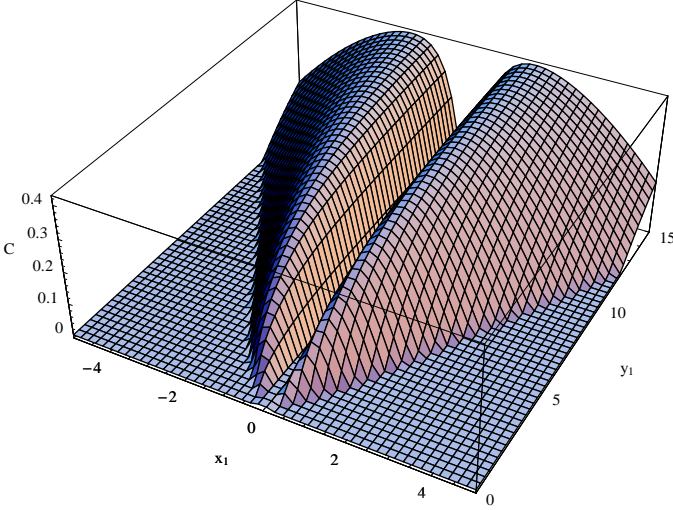
FIG. 2: (color online). The concurrence between cavity 2 and cavity 3 of Fig. 1 as a function of x_1 and y_1. This plot is similar to the Fig. 2 in Ref. [3].

FIG. 3: (color online). The concurrence between cavity 2 and cavity 3 as a function of φ_1 and φ_3. $x_1 = 1.67e^{i\varphi_1}$, $x_3 = 1.67e^{i\varphi_3}$. When $|\varphi_1 - \varphi_3| = (2k+1)\pi$ (k is an integer), the concurrence reaches maximum which is 0.417. The upper left figure is the section at $\varphi_3 = 0$.

where $\Gamma_i = J_i^2 \kappa/(\kappa^2 + \Delta_i^2)$ and Δ_i is the detuning between the central-cavity or a fiber coupler δ_i is the detuning between the driving field of the central cavity in each of the three arms and the polaritonic frequency, assuming different frequencies for the three cavities. $\alpha_i = G_i \tilde{\alpha}_i$, G_i is the coupling of the driving field to the central cavity field in each arm. $\tilde{\alpha}_i$ is the amplitude of the driving field. Note that the photon hopping strengths J_i can be complex numbers, however, the phase of J_i does not affect the entanglement between polaritons, as it can be incorporated into the operators of polaritons and thus amounts to a local unitary operation. Therefore, we will only consider J_i as a real number.

We can now derive the steady state ρ_{ss} by requiring that $\dot{\rho}_{ss} = 0$ in Eq. (1). This is done numerically due to the large numbers of coupled equations involved. Next, we calculate the entanglement between cavity 2 and cavity 3. For this calculation, we first need to trace out the degrees freedom of cavity 1 and then evaluate the concurrence [10] of density matrix of the remaining cavities, using

$$C(\rho_{ss}) = \max\{0, \lambda_1 - \lambda_2 - \lambda_3 - \lambda_4\}, \qquad (3)$$

where λ_i's are, in decreasing order, the nonnegative square roots of the moduli of the eigenvalues of $\rho_{ss}\tilde{\rho}_{ss}$ with

$$\tilde{\rho}_{ss} = (\sigma_1^y \sigma_2^y) \rho_{ss}^* (\sigma_1^y \sigma_2^y), \qquad (4)$$

and ρ_{ss}^* denotes the complex conjugate of ρ_{ss}.

The value for the concurrence between cavity 2 and cavity 3 (denoting it as $C(\rho)$) is plotted against the dimensionless parameters $x_j = \alpha_j(\Delta_j - i\kappa)/(J_j\kappa)$, $y_j = \Delta_j/\kappa$ and $z_j = 1 + \gamma/(2\Gamma_j)$. If we assume $\Delta_1 = \Delta_2 = $
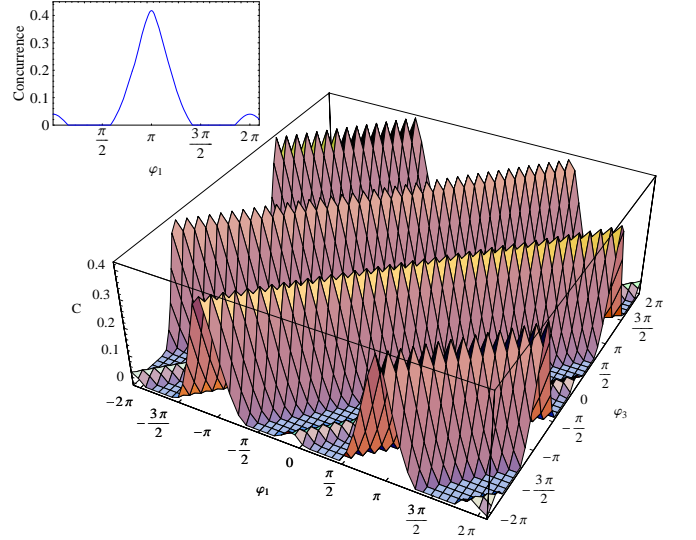
$\Delta_3 = 1.5 \times 10^{14} Hz$ and $\kappa = 10^{13} Hz$ the maximum concurrence can reach 0.402 at $z_1 = z_3 = 1.113$, $z_2 = 114$, and $y_1 = y_2 = y_3 = 15$. These correspond to field amplitudes $\tilde{\alpha}_1 = \tilde{\alpha}_3 = 1.215 \times 10^3$, and couplings $G_1 = -G_3 = 1.0 \times 10^8 Hz$, $G_2 = \tilde{\alpha}_2 = 0$, $\gamma = 10^8 Hz$, $J_1 = J_3 = 1.0 \times 10^{12} Hz$, $J_2 = 3.16 \times 10^{10} Hz$. The effective dissipation rates appearing in the initial Master equation (Eq. 1) are $\Gamma_1 = \Gamma_3 = 4.42 \times 10^8 Hz$ and $\Gamma_2 = 4.41 \times 10^5 Hz$. Theses values are consistent with the parameters used in current or near future technologies, e.g. with coupled toroidal microcavities [5], quantum dots [6] and circuit QED [8]. In Fig. 2, we plot C_ρ for a range of parameters that satisfy $x_1 = -x_3$ and $y_1 = y_3$ and find that the behavior to be similar to the case of two cavity setup in Ref. [3], albeit with a much higher maximum possible entanglement here. We also note here that $\Gamma_2 << \Gamma_1 = \Gamma_3$ and $\Gamma_i \propto J_i^2$, which means that the coupling between the two cavities in question is much weaker than the coupling between each one and the third cavity. Also the state of the polariton in cavity 1 for the maximum entanglement point is $\rho_1 = Tr_{2,3}[\rho] = 0.99|g0\rangle\langle g0| + 0.01|1-\rangle\langle 1 - | \approx |g0\rangle\langle g0|$, which means that the state for the polariton in cavity 1 is almost a pure state at ground energy level. Therefore, it is almost uncorrelated to the polaritons in cavity 2 and cavity 3 which means $\rho \approx |g0\rangle\langle g0| \otimes \rho_{2,3}$. Although this result initially looks counter-intuitive, it can be explained as follows: the maximum entanglement between the two parties, i.e. cavities 2 and 3, in a three party system, is attained when the state of the third party, i.e. cavity 3, nearly factorizes in the combined three party state. The

fact that this is happening for strong relative couplings of $J_{12} \equiv J_1$ and $J_{13} \equiv J_3$ compared to $J_{23} \equiv J_2$ is reminiscent of the behavior of a coherent process taking place. One could dare to observe an analogy here with the case of coherently superposing two initially uncoupled ground states in a Λ type quantum system through an excited state using two classical fields to mediate the interaction.

The last observation is further justified by observing that C_ρ is larger when $x_1 = -x_3$ and $y_1 = y_3$. Taking into account that x_1 and x_3 are functions of the phases of driving fields, these conditions mean that the maximum entanglement is established when the two driving fields have opposite phases. In Fig. 3 we plot the concurrence against the phases of driving fields. Here, $z_1 = z_3 = 1.01$, $z_2 = 11$. When the phase difference is $|\varphi_1 - \varphi_3| = (2k+1)\pi$ (k is an integer), we get again a maximum of 0.417 and an oscillatory behaviour characteristic of the expected coherent effect taking place. In simple words, when the two fields are completely out of phase the entanglement is maximized whereas at phase difference $\pi/2$, the two polaritons are completely disentangled. In all other cases, the amount of entanglement lies somewhere in between.

In Fig. 4, we remove cavity 1 from the configuration of Fig. 1 but with the fiber couplers intact. We then analyze the entanglement between cavity 2 and 3. Optimization of this entanglement gives similar values of the parameters like the ones used above (choose $z = 1.01$); however, the concurrence can reach a maximum of 0.47. Again the dependence $|\varphi_1 - \varphi_3| = (2k+1)\pi$ (k is an integer) is apparent (see Fig. 5). However, if we compare the insets in Fig. 3 and Fig. 5 for the cross-sectional plots of the concurrence for $\varphi_3 = 0$, we see that the plot in Fig. 3 has a narrower peak whereas the plot in Fig. 5 is broad. This implies that the maximum concurrence for configuration in Fig. 4 is substantially more stable against variation in the phases φ_1 and φ_3 than that in Fig. 1.

At this juncture, it is worth emphasizing that we now have three different configurations for comparisons: (i), two cavities with a single driving field in Ref. [3]; (ii), two cavities with three driving fields as in Fig. 4; (iii), three cavities with three driving fields as in Fig. 1. As shown in Fig. 6 when z ranges from 1 to 1.221, the maximum concurrence for configuration (ii) decreases rapidly from 0.48 to 0.285. This rapid decrease means that although configuration (ii) can reach higher entanglement than configuration (i), yet it is more fragile to the dissipation of the environment (parameterized by γ in z). In comparison, the three-cavity setup (which is made by connecting the two side empty cavities with each other through a third cavity doped with an atom) is more robust against the increase of dissipation (only when $z \gtrsim 4.03$, its maximum concurrence drops to be same to that of configuration (i)). Therefore, we conclude that cavity 1 in Fig. 1 not only coherently mediate between cavities 2 and 3, it also
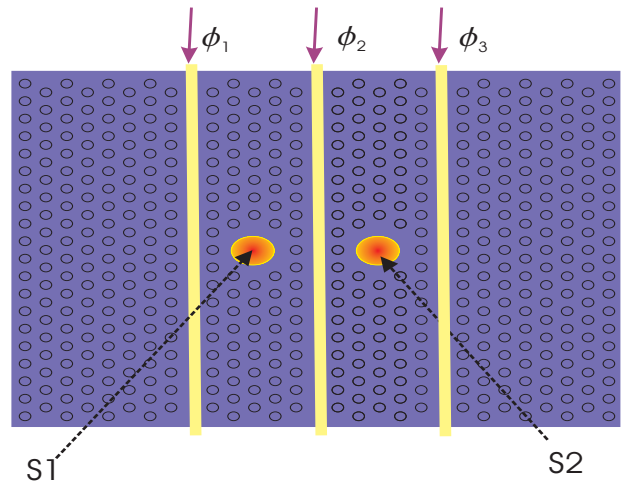

FIG. 4: (color online). Schematic diagram of the two-cavity case in which there are three waveguides carrying the three respective classical laser fields. Note that each waveguide carrying classical fields can also be replaced by fibers in the case of Frabry-Perot cavities or stripline microresonators for circuit QED implementation as before.
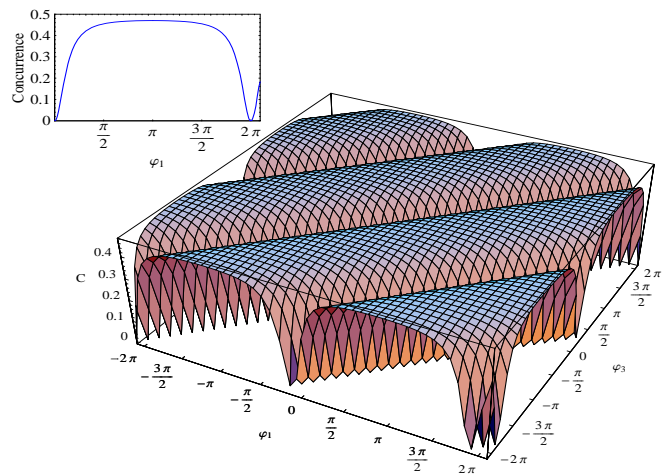

FIG. 5: (color online). The concurrence between two cavities -Fig.4- as a function of φ_2 and φ_3. $x_1 = y_1 = 0$, $x_2 = 5e^{I\varphi_2}$, $x_3 = 5e^{I\varphi_3}$, $\Gamma_2 = \Gamma_3 = 1.316 \times 10^8$ and $\Gamma_1 = 10^{10}$. When $|\varphi_2 - \varphi_3| = (2k+1)\pi$ (k is an integer), the concurrence reaches maximum which is 0.470. The upper left figure is the cross section at $\varphi_3 = 0$.

stabilized the amount of entanglement betwen the two cavities.

One could try to employ entanglement witnesses to detect this entanglement [12]. A witness could be constructed from the density matrix corresponding to the maximum value of the concurrence[3] and then measure it along the corresponding spin directions. In this system to implement the necessary effective spin measurements we can use the usual atomic state measurement techniques employing external laser tuned to the corre-
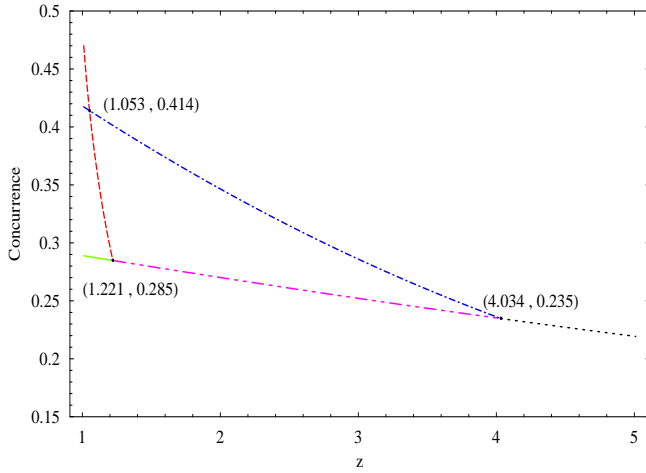
FIG. 6: (color online). The maximum concurrence versus z in three configurations: (i), two cavities with a single coupler in Ref. [3]; (ii), two cavities with three couplers as in Fig. 4; (iii), three cavities with three couplers as in Fig. 1. The solid/dashed line is for configuration (i)/(ii) when $z < 1.221$. The dash dot line is for configuration (iii) when $z < 4.034$. The double dot dash line is for configuration (i) and (ii) when $z > 1.221$. The dot line is for all the three configurations when $z > 4.034$.

sponding polaritonic levels[13]. In these measurements the correlations between the polaritons are transferred to emitted photons and can thus be detected by analyzing the fluorescent photon spectrum. In the following we plot the cross-correlation coefficient $\dfrac{\langle \sigma_2^\dagger \sigma_2 \sigma_3^\dagger \sigma_3 \rangle}{\langle \sigma_2^\dagger \sigma_2 \rangle \langle \sigma_3^\dagger \sigma_3 \rangle}$ for the three cavity scheme in Fig. 1 as function of the phase difference between the driving field 1 and 3 (Fig. 7). The plot is consistent with the concurrence plot in Fig. 3.

In this work, we showed that steady state entanglement in a lossy network of coupled light-matter systems can be coherently controlled through the tuning of the phase difference between the driving fields. We also find that in a closed network of three cavity-atom systems the maximal of entanglement for any pair is achieved even when their corresponding direct coupling is much smaller than their couplings to the third party. This effect is reminiscent of coherent effects found in quantum optics such coherent population transfer between otherwise uncoupled levels through a third level using two classical coherent fields.
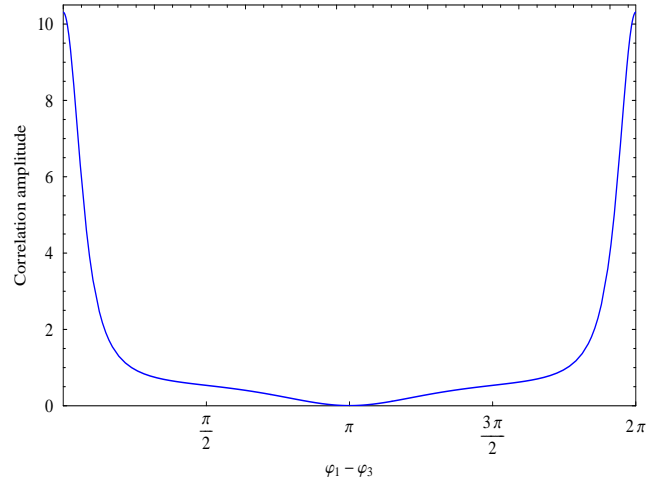
FIG. 7: (color online). (The cross-correlation coefficient $\dfrac{\langle \sigma_2^\dagger \sigma_2 \sigma_3^\dagger \sigma_3 \rangle}{\langle \sigma_2^\dagger \sigma_2 \rangle \langle \sigma_3^\dagger \sigma_3 \rangle}$ for the three-cavity scheme: The minimum value in the cross-correlation coefficient corresponds to maximum concurrence between the cavities.

76 (2007) R05709; M.J. Hartmann, F.G.S.L. Brandao and M.B. Plenio, Nat. Phys., **2** (2006) 849; A. Greentree et al., Nat. Phys., **2** (2006) 856; D. Rossini and R. Fazio, Phys. Rev. Lett., **99** (2007) 186401;M.X. Xuo, Y. Li, Z. Song and C.P. Sun, Phys. Rev. A, **77** 022103 (2008); Y.C. Neil Na *et al.*, Phys. Rev. A, **77** 031803(R)(2008); M. Paternostro, G.S. Agarwal and M.S. Kim, arXiv:0707.0846; E.K. Irish, C.D. Ogden and M.S. Kim, Phys. Rev. A, **77**, 033801 (2008).

[3] D. G. Angelakis, S. Bose and S. Mancini, Eur. Phys. Lett., 85 (2009) 20007.

[4] Dario Gerace. *et al.*, Nature Physics, **5**, 281 (2009); A. Tomadin et al., arXiv:0904.4437.

[5] A. Hattice and J. Vuckovic, App. Phys. Lett. **84**, 191 (2004); A. Badolato *et al* Science, **308**, 1158 (2005); B.S. Song *et al*, Nature Materials **4**, 207 (2005); I. Fushman *et al*, Science, **320** 769 (2008).

[6] D.K. Armani *et al* Nature, **421**, 925 (2003); Takao Aoki. *et al.*, *Nature*, **443**, 671 (2006)

[7] Trupke M. et al., Phys. Rev. Lett., **99**, 063601 (2007). Kivshar Y. S. and Malomed B. A., Opt. Lett., **14** (1989) 1365. Adamova M. S., Zolotovskii I. O. and Sementsov D. I., Opt. Spectrosc., **104** 269 (2008).

[8] J. M. Fink, M. Göppl, M. Baur, R. Bianchetti, P. J. Leek, A. Blais and A. Wallraff, Nature, **454**, 315-318 (2008); Majer J. et al., Nature, **449**, 443 (2007).

[9] J. I. Cirac, R. Blatt, and P. Zoller, Phys. Rev. A **46**, 2668 (1992); Margareta Wallquist, Peter Rabl, Mikhail D. Lukin and Peter Zoller, arXiv:0803.2666v1 [quant-ph] (2008).

[10] W. K. Wootters, Phys. Rev. Lett. **80**, 2245 (1998).

[11] Actually, the maximum value of concurrence 0.47 can be reached at other points, e.g. $x_1 = 0.055$, $y_1 = -0.0001$, $x_2 = -x_3 = 5$, $\Gamma_2 = 5.53 \times 10^5$, $\Gamma_3 = 1.13 \times 10^8$ and $\Gamma_1 = 4.87 \times 10^9$. Here, we only choose a point with relatively high symmetry.

[12] A. G. White, D. F. V. James, W. J. Munro, and P. G. Kwiat, Phys. Rev. A 65, 012301 (2001)

* Electronic address: dimitris.angelakis@gmail.org

[1] D.G. Angelakis, *et al.*, Phys. Lett. A **362**, 377 (2007).

[2] D.G. Angelakis, M.F. Santos and S. Bose, Phys. Rev. A,

[13] M. A. Rowe. *et al.*, Nature, **409**, 791 (2000).